

Impact of M13 Bacteriophage and Administration Routes on Inflammation and Liver Injury in a Mouse Model of Sepsis

Rahimeh Mohseni¹, Sara Soudi¹, Arezou Rahimi¹, Majid Sadeghizadeh², and Arezou Khosrojerdi³

¹ Department of Immunology, Faculty of Medical Sciences, Tarbiat Modares University, Tehran, Iran

² Department of Molecular Genetics, Faculty of Biological Sciences, Tarbiat Modares University, Tehran, Iran

³ Department of Medical Biotechnology, School of Advanced Technologies in Medicine, Tehran University of Medical Sciences, Tehran, Iran

Received: 9 August 2025; Received in revised form: 27 November 2025; Accepted: 28 December 2025

ABSTRACT

Sepsis is a life-threatening condition characterized by a dysregulated immune response leading to organ failure. This study examines the immunomodulatory effects of the M13 bacteriophage in a cecal ligation and puncture (CLP) mouse model of sepsis, comparing intravenous and intraperitoneal delivery routes. Key outcomes included cytokine responses, bacterial burden, organ injury, and survival.

Sepsis was induced using the CLP model. M13 phages were verified by transmission electron microscopy and administered via IV or IP injection. Blood samples were collected at 24 hours, 72 hours, and day 5 for white blood cell, cytokine, and liver enzyme analysis. Bacterial burden was assessed by colony counts, liver injury by hematoxylin and eosin histology, and survival was monitored for 14 days.

CLP induction caused marked increases in WBC counts, cytokines, C-reactive protein (CRP), bacterial load, and liver damage. Following phage treatment, inflammatory markers, bacterial burden, and tissue injury declined substantially. IV administration more effectively reduced systemic inflammation, whereas IP administration provided stronger protection of liver and kidney function and resulted in higher survival rates.

M13 phage therapy demonstrates promising immunomodulatory and organ-protective effects in septic mice. The superior organ protection and survival benefits observed with IP delivery suggest potential translational value for targeted phage administration in sepsis management. Future studies should explore dose optimization, combination therapy, and mechanistic pathways to support clinical development.

Keywords: Bacteriophage; Inflammation; Liver; Sepsis

Corresponding Authors: Sara Soudi, PhD;
Department of Immunology, Faculty of Medical Sciences, Tarbiat Modares University, P.o.Box: 14115-111, Tehran, Iran.
Tel: (+98 21) 8288 3590, Fax: (+98 21) 82884555, Email: srsoudi@modares.ac.ir

Arezou Khosrojerdi, PhD;
Department of Medical Biotechnology, School of Advanced Technologies in Medicine, Tehran University of Medical Sciences, P.o.Box: 14176-13151, Tehran, Iran.
Tel:(+98 21) 4305 2121, Fax: (+98 21) 8899 1117, E-mail: Khosrojerdi.1998@gmail.com

INTRODUCTION

Sepsis is a critical medical condition caused by the dysregulated immune response to infection, leading to organ dysfunction.¹ The progression of sepsis typically follows a 2-phase immune reaction: an initial hyperinflammatory phase, followed by immune suppression, which increases susceptibility to secondary infections. The majority of sepsis-related deaths occur during this immunosuppressive stage.² Affecting approximately 30 million people worldwide each year, sepsis is the leading cause of mortality among critically ill patients, with an alarming annual incidence growth of 9% to 13% and a mortality rate nearing 33%.³

Current management of bacterial sepsis involves fluid resuscitation, hemodynamic monitoring, prompt administration of broad-spectrum antibiotics, and the use of vasopressors when necessary.^{4,5} Despite these interventions, the persistently high mortality rate underscores the urgent need for novel and more effective treatment strategies.

Phage therapy has emerged as a potential alternative to conventional antibiotics, especially with the growing challenge of antimicrobial resistance.⁶ Bacteriophages, which are viruses that selectively infect and destroy bacteria, were independently identified by Felix d'Hérelle and Henry Twort in the early 20th century. Their therapeutic application was first demonstrated in 1919 when a phage cocktail effectively treated a child with bacterial dysentery without causing adverse effects.⁷

Phages replicate within bacterial cells through 2 primary life cycles: the lytic cycle, which results in bacterial cell destruction, and the lysogenic cycle, where the phage integrates its genetic material into the bacterial genome.⁸ The increasing interest in phage therapy is attributed to its unique benefits, such as its ability to penetrate tissues, avoid mammalian immune detection, and modulate immune responses. Phages exert both antibacterial and anti-inflammatory effects by binding to lipopolysaccharides (LPS), reducing excessive reactive oxygen species (ROS) production, and stimulating anti-inflammatory cytokines like interleukin 10 (IL-10).⁹ Among various bacteriophages, the M13 phage—a nonlytic filamentous virus—has demonstrated promising immunomodulatory properties. Recent studies by Safari et al¹⁰ highlighted its ability to influence immune responses in peritoneal macrophages. Additionally,

research by Rahimi et al¹¹ indicated that M13 bacteriophage reduces inflammatory reactions and tissue damage in a sepsis model.

The method of administration significantly impacts the pharmacokinetics, pharmacodynamics, and overall therapeutic efficacy of phage therapy.¹² Intravenous (IV) and intraperitoneal (IP) delivery routes are commonly utilized in preclinical studies. IV administration ensures rapid systemic distribution and complete bioavailability, but it poses solubility and technical feasibility challenges, particularly in small animal models. Conversely, IP administration is widely adopted in experimental studies due to its simplicity and effectiveness for both acute and chronic treatments.¹³

Research on the filamentous M13 phage's therapeutic potential in sepsis is limited, despite evidence of its anti-inflammatory properties. This study addresses key aspects such as administration routes, immune response timing, and long-term survival. Using the cecal ligation and puncture (CLP) model, we evaluate cytokine profiles, organ injury markers, bacterial burden, and 14-day survival. By comparing administration routes and linking immune changes to outcomes, this work enhances our understanding of M13 bacteriophage's role in sepsis management.

MATERIALS AND METHODS

Large-scale Production of Bacteriophage M13

The *Escherichia coli* ER2738 strain used for M13 bacteriophage amplification was provided by Dr Rahbarzadeh and carried an additional low-level kanamycin-resistance plasmid supplied with the strain. Bacteria were initially streaked on LB agar containing tetracycline (10 µg/mL) and incubated overnight at 37°C. To confirm the purity and plasmid maintenance of the provided stock, colonies were restreaked on LB agar supplemented with kanamycin (50 µg/mL). For suspension preparation, a single verified colony was inoculated into 10 mL of 2×YT medium containing tetracycline and grown at 37°C (220 rpm) to mid-log phase (optical density [OD]₆₀₀ = 0.4–0.6). Phage amplification was initiated by adding 20 µL of wild-type M13 to the culture, followed by incubation for 3 hours. The culture was then expanded into 500 mL of 2×YT medium supplemented with tetracycline and kanamycin (50 µg/mL) to ensure plasmid retention during overnight amplification. Following incubation, cultures were

Injection Route of M13 Bacteriophage and Sepsis

centrifuged at $8000 \times g$ for 30 minutes to remove bacterial cells, and the supernatant was further centrifuged at $20\,000 \times g$ for 150 minutes to pellet the phage. The phage pellet was resuspended in phosphate-buffered saline (PBS) and stored for subsequent experiments.

Transmission Electron Microscopy

The structural characteristics of bacteriophage M13 were analyzed using transmission electron microscopy (TEM).

Bacteriophage Titration

To determine the concentration of M13 phages, a serial dilution of the phage stock was performed, reaching a maximum concentration of 10^{13} plaque-forming units (PFU)/mL. For each dilution, 10 μ L of the phage solution was mixed with 90 μ L of *E coli* ER2738 culture in the mid-log phase. The resulting mixtures were spread onto LB agar plates containing tetracycline (10 μ g/mL) and kanamycin (50 μ g/mL), followed by overnight incubation at 37 °C. Plaques formed on the agar were enumerated, and the phage titer was calculated using the standard formula:

$$PFU/mL = \frac{\text{number of plaques}}{\text{Dilution factor} \times \text{Volume [mL]}}$$

Mice

Female C57BL/6 mice (8 to 10 weeks old, 20 to 25 g) were kept in a controlled environment with a 12-hour light-dark cycle. Before experimentation, they underwent a minimum 96-hour acclimation period with free access to food and water.

Study Groups

Mice were randomly assigned to 5 experimental groups ($n = 21$ per group). Of these, 4 mice per group were designated exclusively for the survival analysis and monitored continuously following sepsis induction. These animals were not used for biochemical or histological assessments.

The remaining 17 mice per group were allocated to 3 predefined sacrifice time points to assess the temporal progression of sepsis:

1. 24 hours postinduction: 6 mice
2. 72 hours postinduction: 6 mice
3. Day 5 postinduction: 5 mice

This distribution reflects the known biphasic nature of murine sepsis, in which the first 72 hours correspond

to the acute inflammatory phase, during which animals exhibit rapid clinical deterioration that may limit feasible blood collection. The larger number of mice during the 24-hour and 72-hour time points ensures adequate biological material despite this variability. Allocation of 5 mice to day 5 aligns with ethical considerations and the 3Rs principle to minimize unnecessary animal use.

Treatment Protocols

The treatment groups were as follows:

1. Sham: Underwent all surgical procedures except cecal perforation.
2. CLP: Induced sepsis via CLP.
3. CLP + Imipenem: Septic mice treated with imipenem (25 mg/kg, IP).
4. CLP + Imipenem + M13 Phage (IP): Septic mice receiving both imipenem and M13 phage (10^9 PFU/mL, IP).
5. CLP + Imipenem + M13 Phage (IV): Septic mice administered imipenem along with M13 phage (10^9 PFU/mL, IV).

Imipenem treatment was initiated 30 minutes after sepsis induction and continued every 24 hours for up to 72 hours. M13 phage and imipenem were administered 1 hour apart, with all treatment volumes standardized to 100 μ L. The antibiotic dosage and injection timing were determined based on a prior study conducted in collaboration with this research team.¹⁴

Sepsis Induction

The CLP technique was used to induce sepsis in mice.^{2,15} Anesthesia was administered via IP injection of ketamine (80 mg/kg) and xylazine (4 mg/kg). Following abdominal shaving and disinfection, a midline laparotomy was performed to expose the cecum. The distal half of the cecum was ligated using a 4-0 suture and punctured once with a 22-gauge needle. A small amount of fecal content was gently extruded by applying slight pressure to the cecum before repositioning it within the abdominal cavity. The incision was then sutured closed, and each mouse received a subcutaneous injection of 1 mL saline for fluid resuscitation.

Blood Collection and Sample Allocation

Blood was collected terminally via cardiac puncture under deep anesthesia. Each mouse yielded approximately 800 to 1200 μ L of whole blood, corresponding to 400 to 600 μ L of serum after

centrifugation. To ensure sufficient sample volume for the full biochemical panel, mice at each time point were subdivided into 2 analytic subgroups:

1. $n = 3$ mice per time point per group: Cytokine and liver enzyme analysis.

2. $n = 3$ mice per time point per group: Hematological and biochemical profiling.

All assays were performed in technical triplicate.

White Blood Cells Analysis

Whole blood samples were collected from the retro-orbital sinus and heart at predetermined time points following anesthesia. The samples were immediately transferred to tubes containing an anticoagulant and promptly transported to the laboratory for white blood cell (WBC) quantification using an automated cell counter.

C-reactive Protein Measurement

Serum samples were obtained from 3 mice per group at 24 hours, 72 hours, and 5 days posttreatment. C-reactive protein (CRP) levels were then quantified using enzyme-linked immunosorbent assay (ELISA) kits (Pishtaz teb, Iran).

Bacterial Load Assessment

Bacterial load in the spleen was evaluated at 24 hours, 72 hours, and 5 days postsurgery. Spleen tissue samples (1 mg) from 3 randomly selected mice per time point were homogenized in 1 mL of PBS. Serial dilutions of the homogenate (ranging from 10^{-1} to 10^{-12}) were prepared and plated onto Luria-Bertani (LB) agar (Mirmedia, Iran). Colonies within the 30 to 300 range were counted, and bacterial load was expressed as the logarithmic colony-forming units (CFU) per milligram of spleen tissue.

Cytokine Analysis

Serum samples were collected from 3 mice per group at 24 hours, 72 hours, and 5 days posttreatment. The levels of proinflammatory cytokines, including tumor necrosis factor α (TNF- α) and interleukin 6 (IL-6), as well as anti-inflammatory cytokines such as transforming growth factor β (TGF- β) and IL-10, were quantified using ELISA kits (Karmania Pars Gene, Iran).

Kidney and Liver Function Markers

At 24 hours, 72 hours, and 5 days posttreatment, serum samples were obtained from 3 mice per group to evaluate kidney and liver function. Kidney markers,

including urea and creatinine, as well as liver enzymes-aspartate transaminase (AST), alanine transaminase (ALT), and alkaline phosphatase (ALP)-were measured using an automated clinical chemistry analyzer.

Histopathological Examination

Liver tissues from 3 mice per group were fixed in 10% neutral-buffered formalin for 48 hours, embedded in paraffin, and sectioned at 4 to 5 μ m. Sections were stained with hematoxylin and eosin (H&E) for histopathological evaluation. Liver injury was assessed semiquantitatively using a 0 to 4 grading scale, evaluating key pathological features including hepatocellular necrosis, sinusoidal congestion (hyperemia), inflammatory cell infiltration, and architectural disruption. All slides were scored in a blinded manner by an experienced veterinary pathologist who was unaware of the experimental groups. This approach follows established semiquantitative scoring systems commonly used for inflammatory and injury-related hepatic pathology in murine models.

Survival Study

Survival analysis was conducted over 14 days using 4 mice per group. Mortality was recorded daily, and Kaplan-Meier survival curves were generated using GraphPad Prism v6.

Statistical Analysis

GraphPad Prism (version 6) was utilized for data analysis. The normality of data distribution was evaluated, and results were expressed as mean \pm standard deviation (SD). Group differences were analyzed using a 1-way analysis of variance (ANOVA), followed by Tukey post hoc test for multiple comparisons. Statistical significance was set at $p \leq 0.05$, with significance levels indicated as follows: * ($p \leq 0.05$), ** ($p \leq 0.001$), and *** ($p \leq 0.0001$).

RESULTS

Characterization of Bacteriophage M13 via TEM

Transmission electron microscopy was utilized to assess the morphology and dimensions of bacteriophage M13. The resulting micrographs confirmed its characteristic rod-like shape, with an approximate length of 880 nm and a width of 6.6 nm (Figure 1).

Injection Route of M13 Bacteriophage and Sepsis

WBC Count

A significant increase in WBC count was observed in the CLP group at 24 and 72 hours postsepsis induction compared to the sham group ($p < 0.0001$). However, WBC levels gradually declined over time. In contrast, the groups treated with M13 bacteriophage exhibited a progressive increase in WBC count over time. At the 24-hour mark, the IP M13-treated group demonstrated a more substantial reduction in WBC count compared to the IV M13 group ($p < 0.001$). However, by 72 hours postsepsis induction, WBC levels in the IP M13-treated group had significantly increased compared to the IV M13 group ($p < 0.001$) (Figure 2A).

Serum CRP Levels

CRP levels were significantly elevated in all experimental groups relative to the sham group at 24 hours, 72 hours, and 5 days postsepsis induction, with the highest concentration detected in the CLP group ($p < 0.001$). Over time, a marked decline in CRP levels was observed across all treatment groups ($p < 0.001$). However, no statistically significant difference in CRP concentrations was found between the IP and IV M13-treated groups (Figure 2).

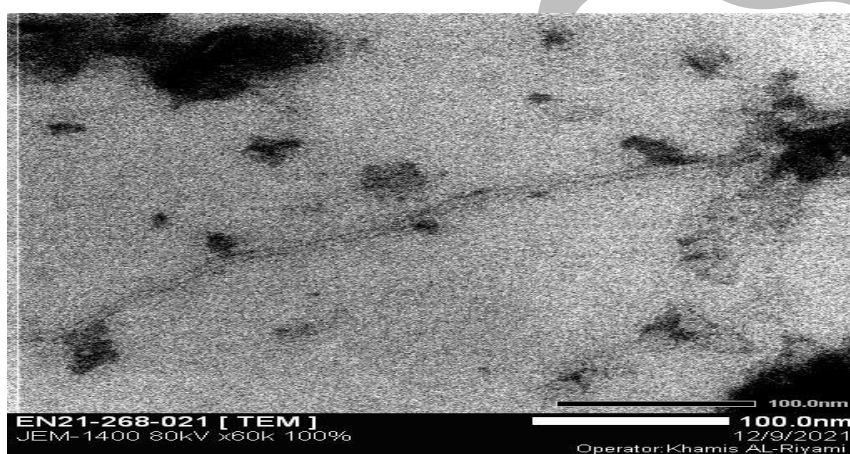


Figure 1. Representative transmission electron microscopy (TEM) micrograph showing the morphology of the M13 bacteriophage.

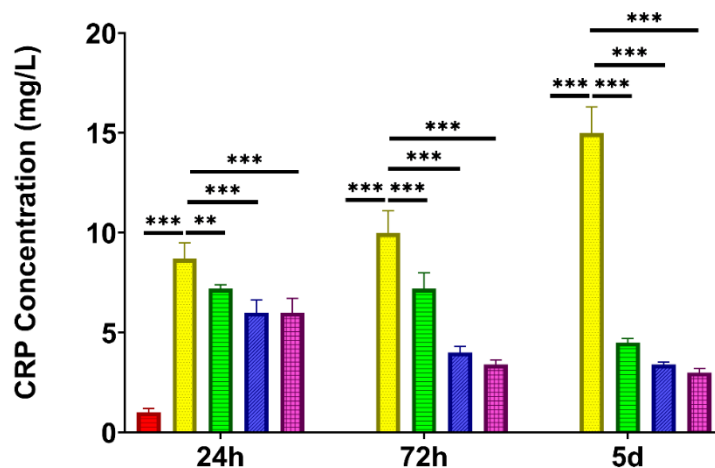


Figure 2. Effects of M13 bacteriophage treatment on serum C-reactive protein (CRP) levels following cecal ligation and puncture (CLP)-induced sepsis. Blood was collected from the hearts of 3 mice in each group at each time point, and serum was isolated. The CRP level was evaluated using enzyme-linked immunosorbent assay (ELISA). After conducting statistical analysis using 1-way analysis of variance (ANOVA) and the Tukey method, the statistical results are presented as the mean \pm standard deviation. p values ranging from < 0.05 to 0.0001 are indicated by different numbers of asterisks (*).

CFU Assessment

Bacterial CFU in the spleen were significantly higher in all groups, particularly in the CLP group, compared to the sham group at 24 hours, 72 hours, and 5 days postsepsis induction ($p < 0.001$). However, all treatment

groups exhibited a notable reduction in bacterial load compared to the CLP group ($p < 0.001$). Despite this overall decrease, no statistically significant difference was observed between the IP and IV M13 treatment groups (Figure 3B).

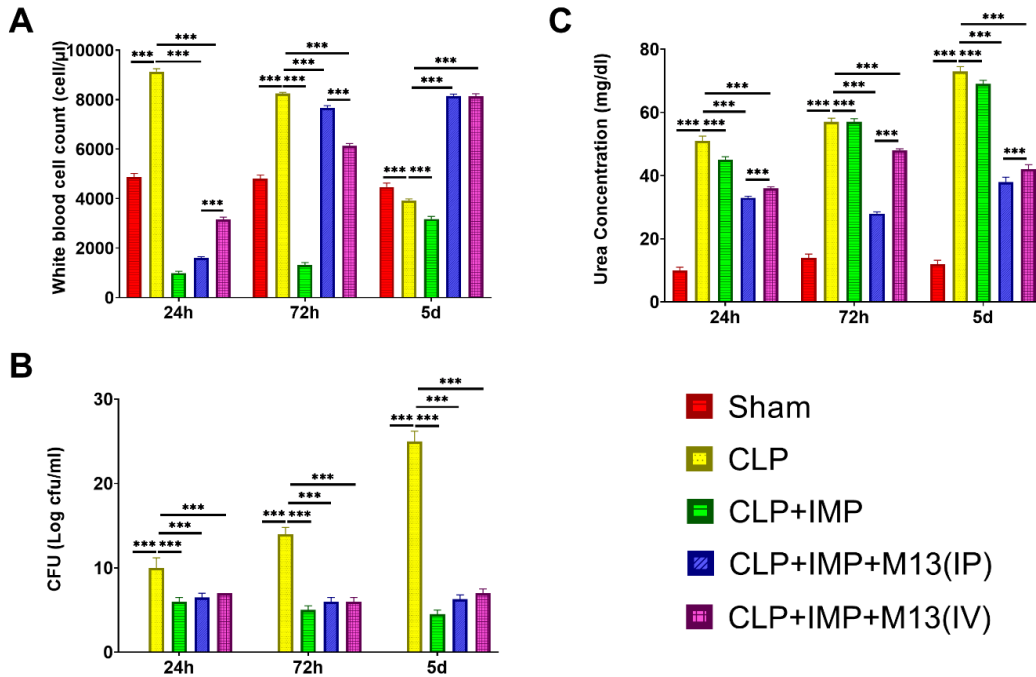


Figure 3. Assessment of white blood cell counts, bacterial load, and kidney injury following cecal ligation and puncture (CLP) and phage treatment. A. Blood was collected from the hearts of 3 mice in each group at each time point, and white blood cell counts were counted using a cell counter. B. In the bacterial load assay, diluted samples were cultured on Luria-Bertani (LB) agar, and colonies were counted to express bacterial load in serum as Log colony-forming units (CFU)/mL. Serum urea levels were measured to evaluate kidney damage. C. After conducting statistical analysis using 1-way analysis of variance (ANOVA) and the Tukey method, the statistical results are presented as the mean \pm standard deviation. p values ranging from < 0.05 to 0.0001 are indicated by different numbers of asterisks (*).

Evaluation of Inflammatory (IL-6, TNF- α) and Anti-inflammatory (IL-10, TGF- β) Cytokines

IL-6 concentrations were significantly elevated in all CLP groups compared to the sham group at all time points, with the highest levels observed in the untreated CLP group ($p < 0.0001$). However, all treatment groups exhibited a substantial reduction in IL-6 levels relative to the CLP group ($p < 0.0001$). The lowest IL-6 concentration was detected in the group receiving M13 bacteriophage via IV injection, showing a statistically significant reduction compared to the IP route at 24 hours and 5 days ($p < 0.0001$) (Figure 4A).

TNF- α levels were markedly higher in all CLP groups than in the sham group, with the highest levels

recorded in the untreated CLP group ($p < 0.0001$). All treated groups showed a significant reduction in TNF- α compared to the CLP group at 24 hours ($p < 0.0001$). Over time, TNF- α levels declined in the CLP group, whereas the CLP + imipenem group exhibited a persistent increase. The IV administration of M13 bacteriophage led to a significant reduction in TNF- α levels compared to the IP route at 24 and 72 hours ($p < 0.0001$). However, by day 5, the IP M13-treated group demonstrated significantly lower TNF- α levels than the IV group ($p < 0.01$) (Figure 4B).

IL-10 levels were significantly elevated in all CLP groups at 24 hours, 72 hours, and 5 days compared to the sham group. Over time, IL-10 levels in the CLP group

Injection Route of M13 Bacteriophage and Sepsis

continued to rise, whereas those in the M13-treated groups exhibited a declining trend. At 24 hours postsurgery, IL-10 levels were significantly higher in the IV M13 group than in the IP group ($p < 0.0001$). However, by 72 hours, this trend reversed, with the IP M13 group showing significantly higher IL-10 levels ($p < 0.0001$). By day 5, no significant differences in IL-

10 concentrations were observed between the 2 administration routes (Figure 4C).

TGF- β levels were significantly higher in all CLP groups compared to the sham group ($p < 0.0001$). At 24 hours, the highest TGF- β levels were observed in the IP M13 group. While TGF- β levels in the CLP group exhibited an increasing trend over time, those in the M13-treated groups showed a gradual decline (Figure 4D).

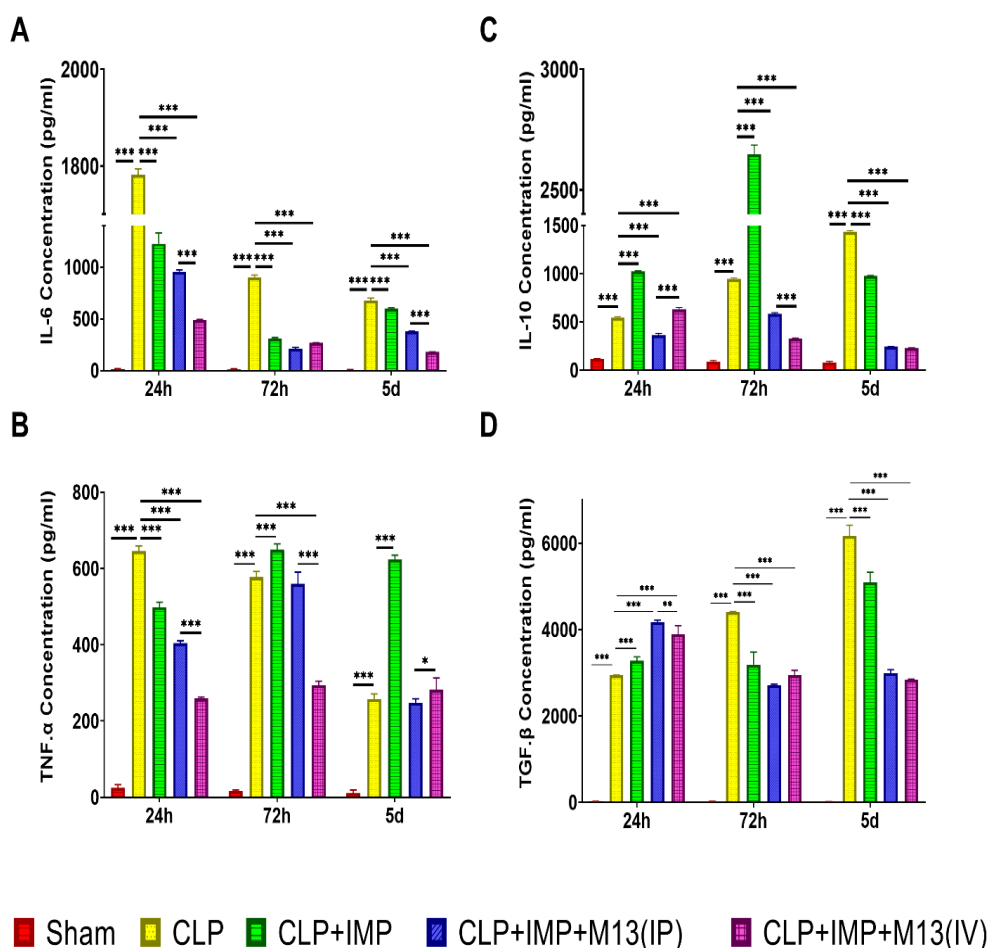


Figure 4. Effects of M13 bacteriophage treatment on serum cytokine levels following sepsis. Serum levels of interleukin-6 (IL-6), tumor necrosis factor- α (TNF- α), interleukin-10 (IL-10), and transforming growth factor- β (TGF- β) were evaluated using enzyme-linked immunosorbent assay (ELISA). After conducting statistical analysis using 1-way analysis of variance (ANOVA), the statistical results are presented as the mean \pm standard deviation. p values ranging from <0.05 to 0.0001 are indicated by different numbers of asterisks (*).

Serum Urea and Creatinine Levels

At all time points, urea levels were significantly elevated in all experimental groups compared to the sham group, with the highest concentrations observed in the CLP group ($p < 0.0001$). However, all treatment groups exhibited a marked reduction in urea levels

relative to the CLP group ($p < 0.0001$). The lowest urea concentration was detected in the IP M13-treated group, showing a statistically significant difference compared to the IV M13 group ($p < 0.0001$) (Figure 2C).

Serum Liver Enzyme Levels

At 24 hours postsepsis induction, AST levels were significantly higher in all groups compared to the sham group ($p < 0.0001$), with a continuous upward trend in the CLP group over time. At both 24 and 72 hours postsurgery, AST levels in the imipenem-treated group were significantly elevated compared to the CLP group; however, by day 5, AST levels in this group showed a decline. In contrast, AST concentrations in the M13-treated groups significantly decreased over time compared to the CLP group ($p < 0.0001$). The lowest AST level was observed in the IP M13-treated group, with a statistically significant difference compared to the IV route ($p < 0.01$) (Figure 5A).

ALT levels were markedly elevated in the CLP group across all time points compared to the sham group. However, treatment led to a significant reduction in ALT concentrations across all treated groups relative to the CLP group ($p < 0.0001$). The only notable difference between the IP and IV M13 treatment groups occurred at the 72-hour time point (Figure 5B).

ALP levels were consistently higher in the CLP group compared to the sham group at all time points observed. The treatment groups exhibited a significant reduction in ALP levels when compared to the CLP group ($p < 0.0001$). No notable differences were observed between the 2 methods of M13 administration, except at the 72-hour mark (Figure 5C).

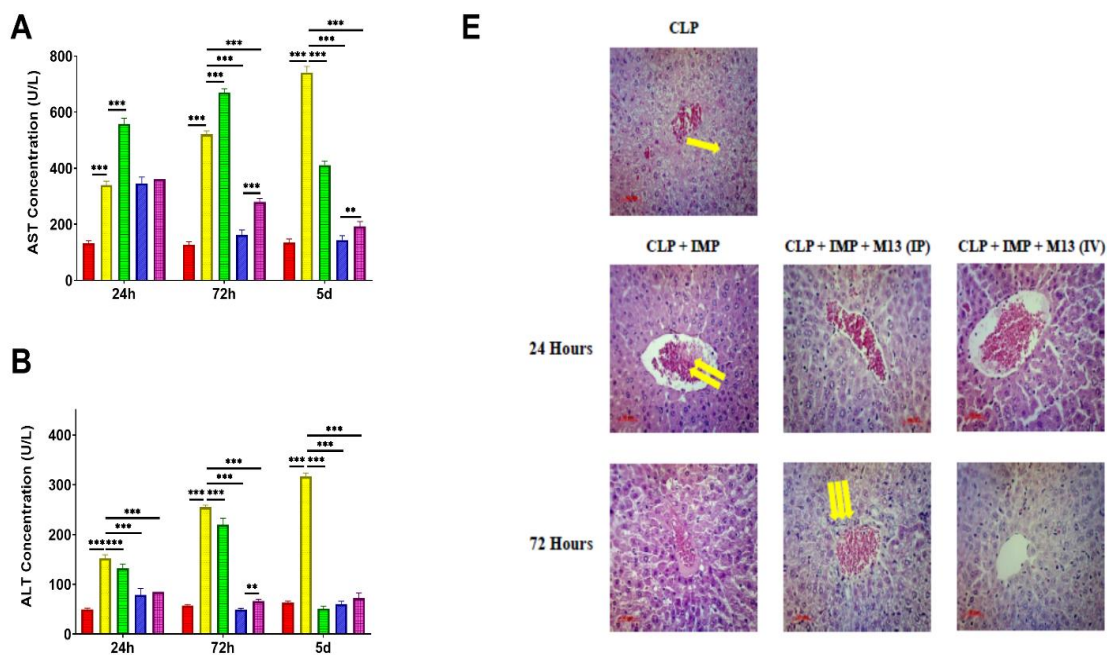
Liver Histopathology Assessment

Liver damage was evaluated based on 4 key pathological features: necrosis, degeneration, inflammation, and hyperemia. Among all groups, the CLP group exhibited the most severe hepatic injury, with damage worsening over time.

At 24 hours postsepsis induction, hepatic steatosis and inflammation were observed across all groups, with the most severe liver damage occurring at the 72-hour mark. Treatment with M13 bacteriophage and imipenem significantly mitigated liver injury compared to the CLP group. Additionally, IP administration of M13 bacteriophage resulted in a more pronounced reduction in liver damage compared to the IV route ($p < 0.001$) (Figure 5D–E).

Survival Rate Analysis

The survival analysis produced the following outcomes: The sham group exhibited a 100% survival rate throughout the 14-day monitoring period, while the CLP group experienced complete mortality within 5 days. By the study's conclusion, the CLP + Imipenem group showed a 60% survival rate. The CLP + Imipenem + M13 (IP) group achieved an 80% survival rate, whereas the CLP + Imipenem + M13 (IV) group reached 70%. No statistically significant difference was observed between the 2 M13 treatment groups, suggesting that both administration routes were equally effective in enhancing survival rates (Figure 6).



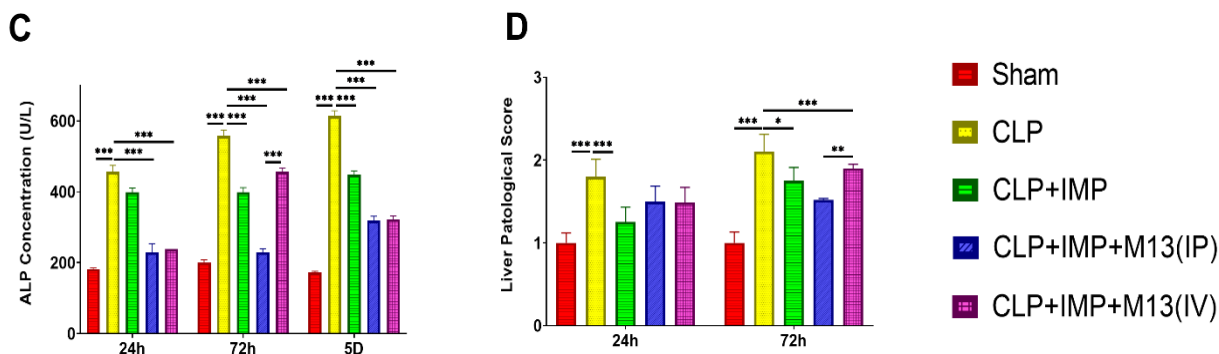


Figure 5. Assessment of liver injury. Blood was collected from the hearts of 3 mice in each group at each time point, and serum was isolated. A–C. Liver enzymes, including alanine aminotransferase (ALT), aspartate aminotransferase (AST), and alkaline phosphatase (ALP), were measured to evaluate liver function. The hematoxylin and eosin (H&E) staining method was utilized for histopathological examinations. D. The pathological score was calculated by a pathologist. E. Single arrow indicates hepatic steatosis, double arrows represent hyperemia, and triple arrows denote inflammatory cell infiltration. After conducting statistical analysis using 1-way ANOVA and the Tukey method, the statistical results are presented as the mean \pm standard deviation. *P* values ranging from <0.05 to 0.0001 are indicated by different numbers of asterisks (*).

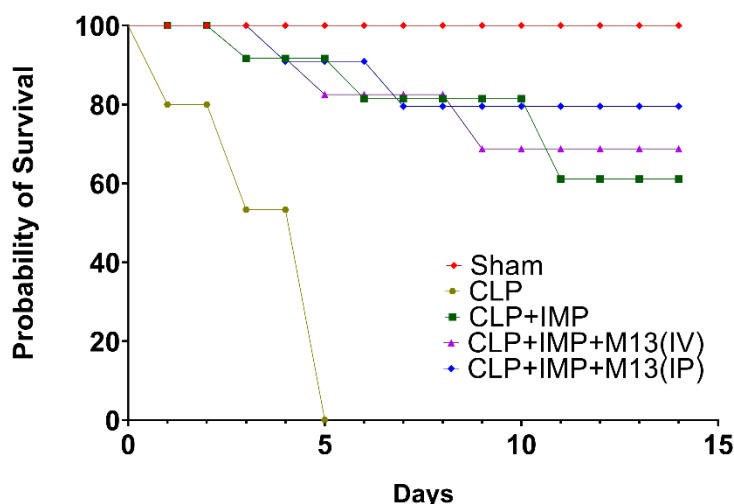


Figure 6. Survival outcomes in septic mice following antibiotic and M13 phage treatments. Kaplan-Meier survival curves for mice monitored over 14 days following cecal ligation and puncture (CLP)-induced sepsis. The sham group maintained 100% survival, whereas the untreated CLP group showed complete mortality within 5 days. The CLP + Imipenem group achieved a 60% survival rate. Combination therapy with Imipenem and M13 phage improved outcomes, with 80% survival in the CLP + Imipenem + M13 (IP) group and 70% survival in the CLP + Imipenem + M13 (IV) group. Statistical analysis was performed using the log-rank (Mantel-Cox) test.

DISCUSSION

Sepsis is a critical condition characterized by an abnormal immune response to infection, resulting in organ dysfunction and high mortality rates.¹⁶ Given the limitations of conventional treatments, phage therapy—particularly with bacteriophage M13—has emerged as a promising alternative due to its notable anti-inflammatory

and antibacterial properties.¹¹ This study assessed the therapeutic potential of M13 bacteriophage in comparison to standard antibiotic treatment with imipenem, focusing on its ability to mitigate sepsis-induced liver injury, systemic inflammation, and mortality.

Previous research has established that sepsis induced via the CLP model leads to a significant increase in bacterial load, accompanied by elevated inflammatory

cytokine levels. This cascade of events contributes to progressive tissue damage, particularly in the liver, and ultimately shortens the lifespan of affected mice.^{11,17,18} Our findings align with these reports, demonstrating a parallel rise in bacterial burden, inflammatory cytokines, and liver damage following sepsis induction.

The potential of phage therapy to enhance anti-inflammatory responses has been widely documented.^{10,11,19} One study reported a significant reduction in leukocyte counts and CRP levels in patients treated with bacteriophages, indicating a decrease in systemic inflammation.²⁰ Similarly, our study showed that M13 bacteriophage therapy effectively reduced CRP levels compared to the CLP group, although no significant difference was observed between IV (IV) and IP (IP) administration routes.

In sepsis, WBC counts typically follow a biphasic pattern: an initial surge due to systemic inflammation, followed by a decline due to apoptosis. Our study confirmed this trend, with WBC counts significantly decreasing over time in the CLP group. However, bacteriophage therapy effectively stabilized WBC levels, countering the decline observed in untreated septic mice. Both IV and IP administration of M13 bacteriophage played a role in regulating WBC fluctuations, with IV injection demonstrating greater efficacy in reducing the initial surge and preventing subsequent depletion. These findings suggest that IV administration may offer superior benefits in controlling inflammation.

Moreover, our results indicated that bacteriophage treatment significantly suppressed the early increase in proinflammatory cytokines while promoting anti-inflammatory cytokines within the first 24 hours. This dual mechanism suggests that bacteriophage therapy not only mitigates acute inflammation but also helps maintain immune balance. As the sepsis model transitioned into an immunosuppressive phase after 5 days, bacteriophage therapy continued to regulate cytokine levels, preventing excessive suppression of the immune response. This effect was particularly pronounced with IV administration, suggesting that it may be more effective in managing inflammation in both the hyperinflammatory and immunosuppressive phases of sepsis.

Various mechanisms have been proposed to explain the immunomodulatory effects of bacteriophages, including their ability to partly attenuate nuclear factor κ B (NF- κ B) signaling, a key driver of proinflammatory

cytokine production.²¹ Bacteriophages can reduce bacterial load and circulating LPS, thereby decreasing Toll-like receptor (TLR) 4 activation;⁹ stimulate IL-10 production,⁹ which directly suppresses NF- κ B; promote a shift from proinflammatory M1 to anti-inflammatory M2 macrophages; and lower ROS levels that otherwise enhance NF- κ B activation.²² Together, these mechanisms help reduce inflammatory cytokines and tissue injury. Although NF- κ B activity was not directly measured in our study, the observed reductions in IL-6, TNF- α , and CRP are consistent with partial inhibition of this pathway.

Additionally, bacteriophages may promote macrophage polarization toward an anti-inflammatory M2 phenotype²³ through several complementary mechanisms. By reducing bacterial load, they decrease exposure to proinflammatory stimuli such as LPS and other pathogen-associated molecules that normally drive M1 activation. Phages can also induce the production of IL-10, a potent anti-inflammatory cytokine that suppresses NF- κ B signaling⁹ and strongly favors M2 differentiation.²⁴ In addition, phage-immune cell interactions may modulate TLR2 and TLR4 signaling, enhance signal transducer and activator of transcription 3 (STAT3) activation, and reduce ROS,^{9,22} collectively creating a cellular environment that supports M2 polarization. Through these pathways, bacteriophages help shift macrophages away from the proinflammatory M1 state and toward an M2 phenotype associated with tissue repair and inflammation resolution.

Uncontrolled inflammation can cause irreversible damage to multiple organs, leading to severe dysfunction or failure.²⁵ Several studies have demonstrated that organ damage, particularly in the liver, lungs, and kidneys, occurs rapidly following sepsis induction via the CLP model.²⁶⁻²⁹ Elevated serum urea and liver enzyme levels—markers of renal failure and liver damage—were observed immediately after sepsis induction, indicating acute inflammation. Our study found that bacteriophage treatment significantly reduced these markers, with IP administration proving particularly effective in preventing tissue injury. These findings align with previous research suggesting that IP injection of bacteriophages facilitates bacterial clearance from the blood and liver, thereby minimizing tissue damage.³⁰ Reduced organ damage and better inflammation control contributed to the increased survival rates observed in the IP bacteriophage-treated group.

IP and IV administration of bacteriophages can lead

Injection Route of M13 Bacteriophage and Sepsis

to different therapeutic outcomes due to variations in pharmacokinetics, biodistribution, and host-phage interactions. IV injection provides rapid systemic exposure but results in quick clearance by the reticuloendothelial system, notably by Kupffer cells in the liver and macrophages in the spleen. This fast clearance reduces the half-life of phages and might limit their antibacterial and immunomodulatory effects, particularly in conditions like sepsis, where immune responses are heightened. In contrast, IP administration delivers phages directly into the peritoneal cavity, allowing for higher local concentrations and slower entry into the bloodstream. This results in prolonged systemic exposure and less immune clearance. IP phages engage with peritoneal immune cells, potentially promoting anti-inflammatory responses. Given that the peritoneum is a major site for bacterial translocation during sepsis, IP delivery may provide more effective bacterial reduction and organ protection than IV methods. These differences in distribution and immune interactions account for the varying therapeutic profiles of IP and IV phage treatments.³¹

Overall, our findings highlight the therapeutic potential of phage therapy as an antimicrobial and immunomodulatory strategy in sepsis. The superior organ protection and survival benefits observed with IP delivery suggest potential translational value for targeted phage administration in sepsis management. Future studies should explore dose optimization, combination therapy, and mechanistic pathways to support clinical development.

This study has several limitations that should be acknowledged. First, although the CLP model provides a clinically relevant representation of polymicrobial sepsis, its severity constrained the experimental design and prevented the inclusion of a phage-only treatment group, limiting our ability to fully isolate the independent effects of M13 bacteriophage from antibiotic-phage interactions. Second, due to the restricted volume of blood obtainable from mice at each time point, certain biochemical and immunological assays were performed on smaller subgroup sizes, which may reduce the statistical power for some endpoints. Additionally, the study focused on short- and intermediate-term outcomes without assessing long-term immunological remodeling or potential phage persistence. Finally, while the IP and IV routes were compared, mechanistic analyses of phage biodistribution and cellular targets were beyond the scope of the present work and warrant further investigation. Despite these

limitations, the findings provide important new insights into the therapeutic potential of M13 bacteriophage in sepsis and lay the groundwork for future mechanistic and translational studies.

Phage therapy presents a promising antimicrobial strategy for modulating inflammatory responses and reducing tissue damage in sepsis. In this study, M13 bacteriophage treatment effectively mitigated inflammation and organ injury, highlighting its potential as an adjunct therapy. While IV administration demonstrated superior control of systemic inflammation, IP injection offered better organ protection and prolonged survival. Future studies should explore the precise mechanisms of bacteriophage-induced immune modulation, particularly its impact on cytokine dynamics within affected tissues.

STATEMENT OF ETHICS

The Tarbiat Modares University Ethics Committee (IR.MODARES.AEC.1401.010) granted the study's ethical approval.

FUNDING

This research received no specific grant from funding agencies in the public, commercial, or not-for-profit sectors.

CONFLICT OF INTEREST

The authors declare no conflicts of interest.

ACKNOWLEDGMENTS

None.

DATA AVAILABILITY

Data will be made available on request.

AI ASSISTANCE DISCLOSURE

Not applicable.

REFERENCES

1. Arina P, Hofmaenner DA, Singer M, editors. Definition and Epidemiology of Sepsis. *Semin Respir Crit Care Med.* 2024;45(4):461-8.

2. Khosrojerdi A, Soudi S, Hosseini AZ, Khaligh SG, Hashemi SM. The combination of mesenchymal stem cell- and hepatocyte-derived exosomes, along with imipenem, ameliorates inflammatory responses and liver damage in a sepsis mouse model. *Life Sci.* 2023;326:121813.
3. Chiu C, Legrand M. Epidemiology of sepsis and septic shock. *Curr Opin Anesthesiol.* 2021;34(2):71-6.
4. Vincent J-L. Current sepsis therapeutics. *EBioMedicine.* 2022;86.
5. Srzić I, Adam VN, Pejak DT. Sepsis definition: What's new in the treatment guidelines. *Acta clinica croatica.* 2022;61(Suppl 1):67.
6. Xu H-M, Xu W-M, Zhang L. Current status of phage therapy against infectious diseases and potential application beyond infectious diseases. *Int J Clin Practice.* 2022;2022(1):4913146.
7. Aswani VH, Shukla SK. An early history of phage therapy in the United States: is it time to reconsider? *Clin Med Res.* 2021;19(2):82-9.
8. Chevallereau A, Pons BJ, van Houte S, Westra ER. Interactions between bacterial and phage communities in natural environments. *Nat Rev Microbiol.* 2022;20(1):49-62.
9. Souza EBD, Pinto AR, Fongaro G. Bacteriophages as potential clinical immune modulators. *Microorganisms.* 2023;11(9):2222.
10. Safari Z, Sadeghizadeh M, Asgaritarghi G, Bardania H, Sadeghizadeh D, Soudi S. M13 phage coated surface elicits an anti-inflammatory response in BALB/c and C57BL/6 peritoneal macrophages. *Int Immunopharmacol.* 2022;107:108654.
11. Rahimi A, Soudi S, Vakiliian S, Jamshidi-Adegani F, Sadeghizadeh M, Al-Hashmi S. Bacteriophage M13 modulates the sepsis-related inflammatory responses and organ damage in a CLP model. *Shock.* 2023;59(3):493-504.
12. Qadir MI, Mobeen T, Masood A. Phage therapy: Progress in pharmacokinetics. *Brazilian J Pharmaceutical Sci.* 2018;54:e17093.
13. Penziner S, Schooley RT, Pride DT. Animal models of phage therapy. *Front Microbiol.* 2021;12:631794.
14. Khosrojerdi A, Soudi S, Hosseini AZ, Khaligh SG, Hashemi SM. Imipenem alters systemic and liver inflammatory responses in CLP-induced sepsis mice in a dose-dependent manner. *Int Immunopharmacol.* 2021;93:107421.
15. Shahi E, Khosrojerdi A, Soudi S, Hosseini AZ. Mesenchymal stem cell-conditioned medium prevents inflammation-induced liver and lung damage in septic mice. *Int Immunopharmacol.* 2024;137:112407.
16. Khosrojerdi A, Soudi S, Hosseini AZ, Eshghi F, Shafiee A, Hashemi SM. Immunomodulatory and therapeutic effects of mesenchymal stem cells on organ dysfunction in sepsis. *Shock.* 2021;55(4):423-40.
17. van der Poll T, Shankar-Hari M, Wiersinga WJ. The immunology of sepsis. *Immunity.* 2021;54(11):2450-64.
18. Wang A, Xiao Z, Zhou L, Zhang J, Li X, He Q. The protective effect of atractylenolide I on systemic inflammation in the mouse model of sepsis created by cecal ligation and puncture. *Pharm Biol.* 2016;54(1):146-50.
19. Abaidullah M, Peng S, Kamran M, Song X, Sher AA, Chen Y, et al. Phageome-based vaccination and human innate immune modulation could be a useful strategy to control human Coronavirus infections. *J Biol Regul Homeost Agents.* 2021;35(3):865-80.
20. Miedzybrodzki R, Fortuna W, Weber-Dabrowska B, Górski A. A retrospective analysis of changes in inflammatory markers in patients treated with bacterial viruses. *Clin Exp Med.* 2009;9(4):303-12.
21. Górski A, Kniotek M, Perkowska-Ptasińska A, Mróz A, Przerwa A, Gorczyca W, et al. Bacteriophages and transplantation tolerance. *Transplant Proc.* 2006;38(1):331-3.
22. Kurzępa A, Dąbrowska K, Skaradziński G, Górski A. Bacteriophage interactions with phagocytes and their potential significance in experimental therapy. *Clin Exp Med.* 2009;9(2):93-100.
23. Secor PR, Michaels LA, Smigiel KS, Rohani MG, Jennings LK, Hisert KB, et al. Filamentous Bacteriophage Produced by *Pseudomonas aeruginosa* Alters the Inflammatory Response and Promotes Noninvasive Infection In Vivo. *Infect Immun.* 2017;85(1).
24. Miernikiewicz P, Kłopot A, Soluch R, Szkuta P, Kęska W, Hodyra-Stefaniak K, et al. T4 phage tail adhesin gp12 counteracts LPS-induced inflammation in vivo. *Front Microbiol.* 2016;7:1112.
25. Wilkinson JD, Pollack MM, Glass NL, Kanter RK, Katz RW, Steinhart CM. Mortality associated with multiple organ system failure and sepsis in pediatric intensive care unit. *J Pediatr.* 1987;111(3):324-8.
26. Hu H, Shi D, Hu C, Yuan X, Zhang J, Sun H. Dexmedetomidine mitigates CLP-stimulated acute lung injury via restraining the RAGE pathway. *Am J Transl Res.* 2017;9(12):5245.
27. Yehya N, Xin Y, Oquendo Y, Cereda M, Rizi RR, Margulies SS. Cecal ligation and puncture accelerates

Injection Route of M13 Bacteriophage and Sepsis

- development of ventilator-induced lung injury. *Am J Physiol Lung Cell Mol Physiol*. 2015;308(5):L443-L51.
28. Senousy SR, Ahmed A-SF, Abdelhafeez DA, Khalifa MMA, Abourehab MA, El-Daly M. Alpha-chymotrypsin protects against acute lung, kidney, and liver injuries and increases survival in CLP-induced sepsis in rats through inhibition of TLR4/NF- κ B pathway. *Drug Des Devel Ther*. 2022;3023-39.
29. Zhang H, Wang W, Fang H, Yang Y, Li X, He J, et al. GSK-3 β inhibition attenuates CLP-induced liver injury by reducing inflammation and hepatic cell apoptosis. *Med Inflamm*. 2014;2014(1):629507.
30. Hung C-H, Kuo C-F, Wang C-H, Wu C-M, Tsao N. Experimental Phage Therapy in Treating *Klebsiella pneumoniae*-Mediated Liver Abscesses and Bacteremia in Mice. *Antimicrob Agents Chemother*. 2011;55(4):1358-65.
31. Ryan EM, Gorman SP, Donnelly RF, Gilmore BF. Recent advances in bacteriophage therapy: how delivery routes, formulation, concentration and timing influence the success of phage therapy. *J Pharm Pharmacol*. 2011;63(10):1253-64.

IMPRESS